Published in final edited form as:
Neurobiol Aging. 2015 February ; 36(2): 1045–1056. doi:10.1016/j.neurobiolaging.2014.11.007.

Effect of IP3R3 and NPY on age-related declines in olfactory stem cell proliferation

Cuihong Jia[a,b] and **Colleen C. Hegg**[a,*]

[a]Department of Pharmacology and Toxicology, Michigan State University, East Lansing, MI 48824, USA

Abstract

Losing the sense of smell due to aging compromises health and quality of life. In the mouse olfactory epithelium (OE) aging reduces the capacity for tissue homeostasis and regeneration. The microvillous cell subtype that expresses both inositol trisphosphate receptor type 3 (IP3R3) and the neuroproliferative factor neuropeptide Y (NPY) is critical for regulation of homeostasis, yet its role in aging is undefined. We hypothesized that an age-related decline in IP3R3 expression and NPY signaling underlie age-related homeostatic changes and olfactory dysfunction. We found a decrease in $IP3R3^+$ and NPY^+ microvillous cell numbers and NPY protein, and a reduced sensitivity to NPY-mediated proliferation over 24 months. However, in IP3R3-deficient mice, there was no further age-related reduction in cell numbers, proliferation, or olfactory function compared to wild-type. The proliferative response was impaired in aged IP3R3-deficient mice when injury was caused by satratoxin-G, which induces IP3R3-mediated NPY release, but not by bulbectomy, which does not evoke NPY release. These data identify IP3R3 and NPY signaling as targets for improving recovery following olfactotoxicant exposure.

Keywords

Olfactory stem cells; olfactory sensory neurons; proliferation; injury; olfactory-mediated behavior

1. Introduction

Losing the sense of smell, whether due to aging or injury, compromises human health and quality of life. More than half of the US population over 65 years exhibits diminished olfactory function, for which no treatments are available. Yet the peripheral olfactory system has a remarkable capacity for neurogenesis, which persists throughout life and which increases significantly following injury. The etiology of age-related decreases in sense of

[*]Corresponding author: 1355 Bogue Street, Room B439 Life Sciences Building, East Lansing, MI 48824, Phone 011-1-517-432-2339, Fax 011-1-517-353-8915.
[b]Present address: Department of Biomedical Sciences, East Tennessee State University, Johnson City, TN 37614 USA

Disclosure statement for authors. The authors have no actual or potential conflicts of interest to declare.

smell has not been elucidated. Several processes may be involved, including cellular senescence (loss of capacity to divide or proliferate) and altered tissue homeostasis (imbalances between cell proliferation, differentiation and death). Alterations in either process can compromise tissue regeneration leading to a decline in olfaction.

In the mature olfactory epithelium (OE), neurogenesis occurs to a small extent to replace a few olfactory neurons that are dying. Multipotent olfactory stem cells, i.e., horizontal and globose basal cells, reside in the basal layers and proliferate and differentiate sequentially into transit amplifying progenitors, immediate neuronal precursor cells, immature neurons and finally mature neurons, moving apically towards the neuronal layer during this process (Caggiano et al., 1994, Calof and Chikaraishi, 1989, Graziadei and Monti-Graziadei, 1978, Leung et al., 2007, Schwartz Levey et al., 1991, Schwob et al., 1994). Cell proliferation and neuronal differentiation in the OE is tightly regulated by multiple signals produced by the stem cell niche, a complex environment that remains to be fully defined (Mackay-Sim and Chuah, 2000). Work from our lab and others localized the neurotrophic factor neuropeptide Y (NPY) predominantly in the subpopulation of microvillous cells that express the IP3R3 receptor (Hegg et al., 2010, Montani et al., 2006) and that have processes extending into the basal cell layer where olfactory stem cells are localized. NPY stimulates basal cell proliferation via a NPY Y1 receptor-activated extracellular signal-regulated kinase signaling cascade (Doyle et al., 2008, Hansel et al., 2001, Jia and Hegg, 2012). A significant reduction in basal cell proliferation occurs in NPY-deficient mice (Hansel et al., 2001) and Y1 receptor-deficient mice (Doyle et al., 2008). Collectively, these data indicate that $IP3R3^{+}$ cells are ideally situated to have a role in promoting olfactory stem cell proliferation by stimulus-induced release of NPY(Jia et al., 2013). In addition, the IP3R3 deficient mouse has significantly reduced olfactory stem cell proliferation in response to injury (Jia et al., 2013). These data indicate that tissue homeostasis and regeneration is dependent, in part, on a microvillous cell that provides an important component of the niche for the resident stem cells: through an IP3R3-mediated mechanism, microvillous cells secrete NPY needed for continual maintenance of the neuronal population (Jia et al., 2013).

Many studies have demonstrated homeostatic changes in the aging OE. There are specific regional decreases in (1) olfactory stem cell proliferation, as measured by BrdU incorporation, (2) numbers of neurons and sustentacular cells, and (3) rate of cell death (Kondo et al., 2010, Loo et al., 1996, Weiler and Farbman, 1997, 1998). The number of neurons expressing NPY in the olfactory bulb decreases with age (Won et al., 2000); however, NPY and NPY receptor expression have not been investigated in the aging OE. We hypothesize that an age-related decline in IP3R3 and NPY signaling may be an underlying cause of age-related homeostatic changes and olfactory dysfunction. To test this hypothesis, we assessed the change in cell populations, proliferative ability, olfactory-mediated behaviors and response to injury in $IP3R3^{+/-}$ and $IP3R3^{-/-}$ mice aged 2–24 months.

2. Materials and methods

2.1 Animals and ethic statement

Mice were bred and maintained in the animal facility in the Life Science building at Michigan State University. All efforts were made to minimize the number of animals used and their suffering. All procedures were conducted in accordance with the National Institutes of Health Guide for the Care and Use of Laboratory Animals as approved by Michigan State University Institutional Animal Care and Use Committee. The IP3R3-tauGFP mouse, in which the first exon of the *Itpr3* gene is replaced by the coding region for a fusion protein of tau and green fluorescent protein, was generously provided by Dr. Diego Restrepo (University of Colorado at Denver, Aurora, CO). As the *Itpr3* gene undergoes biallelic expression, cells in the IP3R3^{+} tauGFP^{-}/IP3R3^{-} tauGFP^{+} mice (denoted IP3R3$^{+/-}$) will express both IP3R3 and GFP, allowing GFP to be used as a marker for IP3R3^{+} cells (Hegg et al., 2010). Cross-breeding the IP3R3$^{+/-}$ mouse generates the IP3R3^{-} tauGFP^{+}/IP3R3^{-} tauGFP^{+} mice (denoted IP3R3$^{-/-}$) that expresses GFP, but not IP3R3. We previously demonstrated that there is neither IP3R3 mRNA, IP3R3 protein (Jia et al., 2013), nor IP3R3 immunoreactivity (Hegg et al., 2010) in the olfactory epithelium of IP3R3$^{-/-}$ mice, supporting a deficiency in IP3R3. Male and female IP3R3$^{+/-}$ and IP3R3$^{-/-}$ mice were used at 2, 6, 12 and 22–26 (denoted as 24) months. Mice were genotyped by PCR analysis of tail DNA using standard methods (Jia et al., 2013). As there are no significant differences in OE tissue homeostasis and response to injury (Jia et al., 2013) nor olfactory function (data not shown) between 2 month old C57BL/6 and IP3R3$^{+/-}$ mice, we used IP3R3$^{+/-}$mice as the control.

2.2 In vivo drug administration and bulbectomy procedure

Anesthetized (4% isoflurane) male and female IP3R3$^{+/-}$ and IP3R3$^{+/-}$ mice (n = 3–6 mice/group) intranasally aspirated NPY (4, 20, 100 nmol/kg), ATP (400 nmol/kg), satratoxin G (100 μg/kg) or an equivalent volume of saline. Unilateral olfactory bulb ablation was performed on male and female IP3R3$^{+/-}$ mice (n = 3–4 mice/group) as described previously (Jia et al., 2010). In order to detect proliferation, mice received two bromodeoxyuridine (BrdU) injections (i.p., total 144 mg/kg) at 6 and 3 hours prior to tissue collection. Tissue was collected 2 days following NPY administration and 6 days following satratoxin G administration or bulb ablation surgery as previously described (Jia et al., 2009).

2.3 Immunohistochemistry

Frozen coronal OE tissue sections (20 μm) were rehydrated with PBS, permeabilized with 0.01–0.3% triton x-100 and blocked with 5% BSA or 10% normal donkey serum. Tissue sections were incubated with goat anti-olfactory marker protein (OMP; 1:1000, Wako Chemicals, Richmond, VA), rabbit anti-cytokeratin 5 (CK5; 1:100, Abcam, Cambridge, MA), mouse anti-mammalian achaete-scute complex homolog-1 (MASH1; 1:30, BD Pharmingen, San Diego, CA), rabbit anti-NPY (1:50–1:150, T-4069; Bachem, Torrance, CA) or rat anti-BrdU antibody (1:100, Abcam, Cambridge, MA) overnight at 4 °C . Immunoreactivity was detected by TRITC- or Cy3-conjugated donkey anti-goat, -mouse or -rabbit immunoglobin (1:50 or 1:200, Jackson ImmunoResearch Lab, West Grove, PA). The nuclei were counterstained with Vectashield mounting medium for fluorescence with DAPI

(Vector Laboratory, Burlingame, CA). For detection of CK5 and MASH1, antigen retrieval was performed before permeabilization by placing sections in a citrate buffer (pH=6) or HCl (2 M) and heated in a microwave oven (700 W) at low power for 2 × 6 min and cooled for 20 min. Following this procedure, DAPI nuclear staining did not work very well, but we could delineate the basement membrane on which the horizontal basal cells reside. For detection of BrdU, tissue sections were incubated in 2 M HCl for 30 min at 65 °C to denature DNA before blocking as described above. NPY immunoreactivity was amplified using a tyramide signal amplification kit (Molecular Probes, Eugene, OR) according to the manufacturer's instructions. Immunoreactivity was visualized on an Olympus FV1000 confocal laser scanning microscope (Pleasant Valley, PA). Antibody specificity was examined by omitting the primary antibody or secondary antibody. No immunoreactivity was observed in any of the controls.

The number of GFP^+, $CK5^+$, $MASH1^+$, $BrdU^+$, NPY^+ or $CK5^+/BrdU^+$ in the ectoturbinate 2 and endoturbinate II on three consecutive coronal sections of OE were counted by an experimenter blinded to the treatments and genotypes (n = 3–6 mice/group). The ectoturbinate 2 and endoturbinate II are entirely comprised of olfactory epithelium and the linear length of these turbinates was determined by tracing the basement membrane using MetaMorph software (Molecular Devices, Sunnyvale, CA). Data was normalized to the length of OE on which the immunopositive cells were scored and expressed as number per linear millimeter OE. To further examine the GFP^+ cell localization in the OE, a 200 μm OE section from a 2 month old $IP3R3^{+/-}$mice was scanned using an Olympus FV-1000 2-Photon confocal microscope (Pleasant Valley, PA; 488 nm ex, 510 nm em, 1.05 NA 25× water objective with 1 μm step).

The percent volume density of OMP^+ cells was measured by STEPanizer software (www.stepanizer.com (Tschanz et al., 2011). Briefly, a small 130×130 μm 144-point overlay was randomly placed (total area analyzed = 16900 μm^2/location) in 6 locations of ectoturbinate 2 and 4 locations of endoturbinate II in three consecutive coronal OE sections per animal. The volume density of OMP^+ cells was determined by manual point counting and expressed as the percentage of the ratio of the number of test points hitting OMP^+ cells, divided by the total number of points hitting the OE.

2.4 ELISA and quantitative RT-PCR of NPY

Anesthetized (65 mg/kg ketamine + 5 mg/kg xylazine, ip) $IP3R3^{+/-}$ mice of both sexes (n = 4 mice/group) were decapitated, the heads were cut sagittally along the midline, and the OE from each side was dissected and stored separately at −80 °C . One side of the OE was used to measure NPY protein levels by ELISA and the other side was used to measure mRNA of NPY by quantitative RT-PCR. For NPY protein analysis, OE tissues were processed following the protocol described previously (Jia et al., 2009) and the levels of NPY protein were measured using a NPY ELISA kit (Peninsula Laboratories, San Carlos, CA) following manufacturer's protocols. Data is reported as pg NPY/μg OE protein as measured using a BCA protein assay kit (Pierce Biotechnology, Rockford, IL). For NPY mRNA analysis, the total RNA was extracted from OE homogenates (TRIzol reagent, Invitrogen, Carlsbad, CA) and used at final concentration of 100 ng/μl. The reverse transcription was performed with 2

μg of total RNA using High Capacity cDNA Reverse Transcription kit (Applied Biosystem, Foster City, CA) following manufacturer's protocols and GeneAmp PCR System 9700 (Applied Biosystem, Foster City, CA). Reaction products (250 ng/μl) were used for quantitative real time-PCR by 7500 real-time PCR system (Applied Biosystem, Foster City, CA). The NPY and internal control gene mouse GAPDH were amplified by Taqman Gene Expression Master Mix and Taqman primers (GAPDH, Mm99999915_g1, NPY, Mm03048253_m1, Applied Biosystem, Foster City, CA) following manufacturer's protocols. Expression of NPY and GAPDH mRNA were determined in triplicates. NPY mRNA relative expression was presented by the Δ cycle threshold (ΔC_T) as C_T of NPY-C_T of GAPDH.

2.5 Olfactory behavior tests: buried food test and habituation/dishabituation test

For the buried food test, a trial was administered every other day for 7 days (4 trials total). Mice of both sexes (n = 12–16 mice/group) were fasted 16–18 h prior to each trial day. For trials 1–3, a mouse was first acclimated in a cage filled only with fresh wood chip bedding for 5 minutes, transferred to a second cage for 5 minutes and then to a third cage that contained a piece of sugary cereal that was buried beneath the bedding in a randomly selected location. On the 4th trial, the sugary cereal was placed on the surface of bedding. The latency to uncovering and eating the buried food was measured. Trial 1 measures naïve olfactory-mediated finding, trial 2 and 3 examine improvement based on positive reinforcement received in the previous trials and indicate olfactory-mediated learning and memory, while trial 4 with visible cereal is used to assess locomotor ability. Only mice that could find the buried food within 5 min and eat the food were chosen for data analysis. The average improvement factor was calculated as ∑(T1/T3)/n (Le Pichon et al., 2009).

The habituation/dishabituation test was performed and analyzed as described previously (Le Pichon et al., 2009). Briefly, mice of both sexes (n = 12–16 mice/group) were acclimated in the test cage for 30 min with a clean dry cotton applicator inserted through the hole on the cage lid prior to the beginning of trials to reduce novelty-induced exploratory activity during the subsequent trials. Distilled water (100 μl), peppermint extract or almond extract (100 μl of 1:100 diluted with distilled water, McCormick & Co., Hunt Valley, MD) were applied to a cotton applicator that was then inserted through the hole on the cage lid. For each trial an odorant was delivered for 2 min with a 30 second delay before the next trial began. The testing consisted of 3 trials of distilled water, 3 trials of peppermint then 3 trials of almond. Investigation was defined as active sniffing within a 1 cm radius of the cotton applicator with the snout oriented towards the applicator. The cumulative investigation time during the 2 min odorant presentation was recorded by a single observer blind to genotypes. Investigation time for trial 1 was calculated for each animal as $\sum[(\text{Trial } 1_{\text{distilled water}} + \text{Trial } 1_{\text{peppermint}} + \text{Trial } 1_{\text{almond}})]/3$. As there was a significant difference in investigation times of trial 1 across ages, the investigation times of the three trials for each odorant and for each animal were normalized to the maximal time for that odorant. Thus, for each animal, the maximal investigation time for each odorant was 1 and shorter investigation times were expressed as a fraction of 1. Odorant habituation was assessed by analyzing the investigation times of repeated exposure to the same odorant. All normalized trial 1 investigation times were averaged for each animal ([∑normalized Trial $1_{\text{distilled water}}$ +normalized Trial

$1_{peppermint}$ +normalized Trial 1_{almond}]/3) and likewise for trial 2 and trial 3. The habituation index for each animal was calculated as ∑[(1-normalized Trial $3_{distilled\ water}$)+(1-normalized Trial $3_{peppermint}$)+(1-normalized Trial 3_{almond})]/3. The cross-habituation index for each animal was calculated as ∑[(normalized Trial $1_{peppermint}$-normalized Trial $3_{distilled\ water}$)+(normalized Trial 1_{almond}-normalized Trial $3_{peppermint}$)]/2.

2.6 Statistical analysis

Student's t-test, and one-way ANOVA followed by the Newman-Keul post hoc test was performed using Prism 5 (Graphpad Software, San Diego, CA). Two-way ANOVA or repeated-measures two or three-way ANOVA was performed followed by the Newman-Keul post hoc test when the number of groups less or equal to three or the Tukey/Kramer Procedure post-hoc test when the number of groups was more than three using GB-Stat v9.0 (Dynamic Microsystems, Inc., Silver Spring, MD).

3. Results

3.1 Age-dependent reduction in the number of IP3R3$^+$ cells in the OE

IP3R3$^+$ microvillous cells in the OE predominantly express NPY (Kanekar et al., 2009, Montani et al., 2006). Our previous study showed that IP3R3-dependent NPY release mediates an increase in basal cell proliferation in mouse OE following injury (Jia et al., 2013). We hypothesized that age-related changes in the stem cell microenvironment, especially to the IP3R3$^+$-NPY$^+$-microvillous cell, reduces the capacity to maintain tissue homeostasis and undergo regeneration. We first visualized and quantified IP3R3$^+$ cells in the OE of IP3R3$^{+/-}$mice using GFP as a marker (Figure 1). GFP$^+$ cells were broadly and evenly distributed in the whole ectoturbinate 2 of OE at 2 months old (Figure 1C–F). However, the number of GFP$^+$ cells significantly decreased over 24 months (Figure 1G–K, $p < 0.05$, 2 vs. 6, 12 and 24 months, 6 vs. 24 months), indicating an age-dependent reduction in IP3R3$^+$ cells in the OE. An accumulation of granules containing autofluoresent lipofuscin-like proteins can be observed at 24 months (Figure 1J). Lipofuscin-like proteins accumulate in aging cells and have been demonstrated in the OE of aged rodents (Naguro and Iwashita, 1992). In addition, there is an age-dependent increase in the length of the OE over time (Figure 1L, $p < 0.001$, 2 vs. 6, 12 and 24 months, 6 vs. 24 months, 12 vs. 24 months). The number of GFP$^+$ cells was normalized to the length of OE (Figure 1K), therefore, it is possible that the age-dependent reductions in GFP$^+$ cells we observed could be due to the increase in OE length. However, the number of GFP$^+$ cells decreased by 24%, 46% and 61% at 6, 12 and 24 months, respectively, compared to 2 months, while the length of OE only increased 13%, 13% and 25%, respectively. Taken together, these data indicate an age-dependent reduction in IP3R3$^+$ cells occurs in mouse OE.

3.2 Age-dependent reduction in the number of NPY$^+$ cells and NPY protein levels in the OE

We next investigated whether the age-dependent reduction of IP3R3$^+$ cells in the OE affected the number of NPY$^+$ cells in the ectoturbinate 2 and endoturbinate II at 2 and 24 months old. At 2 months old, 90.1 ± 2.0% of the NPY$^+$ cells were NPY$^+$-GFP$^+$ microvillous cells (mean ± SD; n = 3 mice). The number of NPY$^+$ cells was significantly reduced at 24 months compared to 2 months (Figure 2A–C, $p < 0.05$). Consistently, the level of NPY

protein in the OE at 24 months was significantly decreased compared to 2, 6 and 12 months old (Figure 2D, $p < 0.01$). However, the mRNA levels of NPY in the OE were comparable among ages (Figure 2E, $p > 0.05$). These data indicate that expression of the neuroproliferative factor NPY decreases significantly with age, likely through post-transcriptional regulation.

3.3 Age-dependent reduction in the numbers of olfactory stem cells, olfactory stem cell proliferation and olfactory sensory neurons in the OE

Age-related alterations in homeostasis are associated with reductions in olfactory stem cell proliferation and stem cell numbers, and alterations in olfactory sensory neurons (Loo et al., 1996). We examined homeostasis in IP3R3$^{+/-}$ at different ages by evaluating the numbers of basal cells, basal cell proliferation and olfactory sensory neurons. The numbers of horizontal basal cells expressing cytokeratin 5 (CK5) and globose basal cells expressing mammalian achaete-scute complex homolog-1 (MASH1) were significantly reduced at 6, 12 and 24 months compared to those at 2 months (Figure 3A–D, $p < 0.01$ or 0.05). There was no significant difference in the numbers of MASH1^{+} and CK5^{+} cells at 6, 12 and 24 months in the OE, indicating that the main significant decrease in basal cell numbers occurs after 2 months, a time when tissue expansion is normally completed. The numbers of BrdU-labeled proliferating basal cells were significantly reduced at 12 and 24 months compared to 2 or 6 months (Figure 3E–F, $p < 0.001$), confirming age-dependent reduction of basal cell proliferation in the OE. In the OE of both 2 and 24 month mice, less than 3% of the BrdU-labeled proliferating basal cells were CK5^{+} horizontal basal cells (Figure 3G–H), indicating that the globose basal cell population is the cell that undergoes proliferation in both young and aged OE under physiological conditions. The volume density of OMP^{+} cells in the OE was significantly reduced at 12 and 24 months (Figure 4A–B, $p < 0.01$). The loss of OMP^{+} olfactory sensory neuron axons in the olfactory bulb was also observed in 24 month mice (Figure 4C–D), indicating an age-dependent reduction in olfactory sensory neurons.

To determine the effect of IP3R3-mediated NPY release on the aging process and the ability to undergo proliferation, we examined the complement of cell types and proliferation in the OE of 12 and 24 month IP3R3$^{+/-}$ and IP3R3$^{-/-}$ mice (Figure 5). There were no differences between genotypes in the numbers of CK5^{+} basal cells, MASH1^{+} progenitor cells or BrdU incorporation at 12 and 24 months (Figure 5A–C; $p<0.05$). The neuronal density was also not altered between genotype at 12 and 24 months (Figure 5D; $p<0.05$). These data indicate that IP3R3-dependent processes such as NPY expression and subsequent release do not play a role in the reduction in proliferation observed during aging.

3.4 Age-dependent reduction in olfactory-mediated functions

We measured olfactory-mediated functions in IP3R3$^{+/-}$ mice at different ages using the buried food test and olfactory habituation/dishabituation test. In the buried food test, the latencies to find a buried food in fasted mice were measured 3 times (Trial 1–3). The latency of trial 1 at 24 months was significantly increased compared to 2, 6 and 12 months (Figure 6A), indicating the naïve olfactory-mediated food finding ability is impaired in aged mice. In order to examine the improvement factor from trial 1 to 3, we calculated the ratio of latency in trial 1/latency in trial 3 (Figure 6B). There was a significant age-dependent

reduction in the improvement factor ($p < 0.05$ at 2 vs. 6, 12 and 24 months), indicating an age-dependent impairment of olfactory-mediated learning and memory. The longer latencies in aged mice could be due to a reduction in locomotor ability. However, the latencies in trial 4 with visible food were similar among ages (Figure 6C, $p>0.05$), indicating that the impairment in olfactory-mediated food finding, learning and memory in aged mice is due to a deficiency in odorant detection and not locomotor ability.

We performed the olfactory habituation/dishabituation test to measure olfactory perception and discrimination in IP3R3$^{+/-}$ mice at different ages. This behavior test measures novel odorant investigation in the first trial and odorant habituation by exposure to the same odorant in the next 2 trials, and odorant dishabituation by exposure to a different odorant. We measured novel odorant investigation by pooling the investigation time of trial 1 for each odorant (water1, peppermint1 and almond1) at each age group (Figure 6D). The investigation time at 24 months was significantly less than at 2 and 6 months ($p < 0.01$ or 0.05), indicating either impairment in odorant detection or a reduced motivation to investigate in aged mice (24 months). We next assessed odorant habituation over repeated odorant exposures. In general, all mice showed decreases in investigation times in trials 2 and 3 (habituation; Figure 6E) and an increase in investigation times with novel odorant presentation, i.e., trial 1 (dishabituation; Figure 6E). There were no significant differences in the habituation index among ages (Figure 6F; $p>0.05$), indicating all mice have a similar ability to habituate to repeated odorant exposure. The ability to discriminate odorants was assessed using the cross-habituation index (Figure 6G). The cross-habituation index at 24 months was significantly lower than those at 2 and 12 months ($p < 0.05$ or 0.01, respectively), indicating that aged mice (24 months) have an impaired ability to discriminate between different odorants.

To determine the effect of IP3R3-mediated NPY release on the aging process and olfaction, we performed the buried food test and the habituation/dishabituation assays with 12 and 24 month IP3R3$^{+/-}$ and IP3R3$^{-/-}$ mice (Figure 7). There were no differences found between genotype in assessment of the buried food test in naïve olfactory-mediated food finding ability (Figure 7A; $p>0.05$), improvement factor (Figure 7B; $p>0.05$) or in mobility (Figure 7C; $p>0.05$). There were also no differences found between genotype in odorant detection (Figure 7D; $p>0.05$), the ability to habituate to an odorant (Figure 7E; $p>0.05$), and the ability to discriminate between odorants (Figure 7F; $p>0.05$). Collectively these data indicate that IP3R3-mediated processes do not play a role in the reduction in olfactory ability observed during aging.

3.5 Trophic factor-stimulated basal cell proliferation is reduced in aged OE

We investigated the effects of NPY on olfactory stem cell proliferation in the OE of IP3R3$^{+/-}$ mice at different ages. Mice intranasally aspirated vehicle or NPY (4 nmol/kg) and basal cell proliferation was quantified by measuring BrdU-incorporation in the ectoturbinate 2 and endoturbinate II OE. In vehicle-treated animals, the number of BrdU^{+} cells at 24 months was significantly reduced compared to 2 and 6 months and the number of BrdU^{+} cells at 12 months was significantly reduced compared to 2 months (Figure 8A–B, vehicle treatment: $p < 0.05$, 12 vs. 2 months, 24 vs. 2, 6 months). These data confirm our previous

observation of an age-dependent reduction in basal cell proliferation in the OE under physiological conditions (Figure 3E–F). NPY significantly increased $BrdU^+$ cells in the OE at 2 and 6 months compared to the corresponding vehicle ($p < 0.05$) but not at 12 and 24 months ($p > 0.05$), indicating NPY at 4 nmol/kg is unable to promote basal cell proliferation in the OE of aged mice. When the concentration of NPY administered was increased (100 nmol/kg) the number of $BrdU^+$ cells in 12 month old mice significantly increased (Figure 8C, $p < 0.01$ compared to vehicle, 4 nmol/kg and 20 nmol/kg), indicating the olfactory stem cells in the OE of aged mice are still responsive to the neuroproliferative effects of NPY, but need a higher concentration. A reduction in basal cell proliferation was also observed in aged mice that had aspirated a different trophic factor, ATP (Figure 8D). ATP significantly increased BrdU-labeled basal cell proliferation in the OE of 2 month ($p < 0.01$) but not 24 month mice ($p > 0.05$). Collectively, these data indicate trophic factor-stimulated proliferation is reduced in aged mice.

3.6. The response to injury is impaired in aged $IP3R3^{+/-}$ and $IP3R3^{-/-}$ mice

We examined the effect of age on the regenerative response of $IP3R3^{+/-}$ and $IP3R3^{-/-}$mice following OE injury, an event that requires a significant population of olfactory stem cells to proliferate and differentiate to replace dying olfactory sensory neurons. We used 2 methods to cause injury: (1) administration of satratoxin G that causes ATP-induced IP3R3-dependent NPY release (Jia et al., 2011) and (2) bulbectomy that does not cause ATP-activated IP3R3-mediated NPY release (Jia et al., 2013, Jia et al., 2010). $IP3R3^{+/-}$ and $IP3R3^{-/-}$ mice at 2, 6, 12 and 24 months old intranasally aspirated vehicle or satratoxin G (100 μg/kg) or underwent a unilateral bulbectomy, and BrdU-incorporation was quantified in the OE at 6 days post-aspiration or surgery. Consistent with previous observations (Figure 3E–F, 6C), there were age-dependent reductions in $BrdU^+$ cells in the control OE (vehicle-treated or unlesioned side of bulbectomy) of both $IP3R3^{+/-}$ and $IP3R3^{-/-}$ mice (Figure 9, circles). In addition, the numbers of $BrdU^+$ cells in the OE of controls (vehicle, unlesioned) were comparable between $IP3R3^{+/-}$ and $IP3R3^{-/-}$ mice at all ages checked (Figure 9, circles). Following satratoxin G treatment or bulbectomy, the number of $BrdU^+$ cells in 12 and 24 month mice was significantly reduced compared to 2 and 6 month mice in both $IP3R3^{+/-}$ and $IP3R3^{-/-}$ mice (Figure 9A–B, $*p < 0.01$), indicating an age-dependent reduction in basal cell proliferation following injury. The number of $BrdU^+$ cells in satratoxin G-treated $IP3R3^{+/-}$ mice was significantly greater than the respective vehicle-treated $IP3R3^{+/-}$ mice at all ages checked (Figure 9A; #, $p < 0.05$ v. saline vehicle), indicating the $IP3R3^{+/-}$ mice at all ages (2–24 months) respond to satratoxin G injury by significantly increasing basal cell proliferation. In satratoxin G-treated $IP3R3^{-/-}$ mice, however, the number of $BrdU^+$ cells was significantly increased only in the 2 month, but not the 6, 12, and 24 month old $IP3R3^{-/-}$ mice (Figure 9A; #, $p < 0.01$ v. saline vehicle). These data indicate that the regenerative response to satratoxin G-induced OE injury is significantly impaired in aged $IP3R3^{-/-}$ mice. Furthermore, the number of $BrdU^+$ cells in the OE of satratoxin G-treated $IP3R3^{-/-}$mice was significantly lower than those in satratoxin G-treated $IP3R3^{+/-}$ mice at 2 and 6 months (Figure 9A; +, $p < 0.05$). These results indicate that IP3R3 has an important role inducing basal cell proliferation in the OE of young and old mice following satratoxin G injury. In contrast to satratoxin G-treated mice, bulbectomy significantly increased BrdU incorporation in $IP3R3^{+/-}$ and $IP3R3^{-/-}$ mice at all ages

(Figure 9B; #, $p < 0.05$ vs. respective unlesioned side), indicating both aged IP3R3$^{+/-}$ and IP3R3$^{-/-}$ mice have a similar ability to respond to bulbectomy. Taken together, data from two injury models indicate that the response to injury is impaired in aged mice and that the injury response to satratoxin G, that involves release of NPY, is more compromised in the OE of aged IP3R3$^{-/-}$ mice than following bulbectomy, that does not involve the release of NPY.

4. Discussion

We investigated the aging process in the OE, specifically regarding NPY levels, the response of olfactory stem cells to NPY, olfactory-mediated functions, and OE tissue homeostasis and the response to trophic factors and injury. We found in mouse OE that there are age-dependent reductions in IP3R3^{+} cells, NPY^{+} cells, NPY protein levels, olfactory stem cells, stem cell proliferation, olfactory sensory neurons and olfactory-mediated functions. In addition, the olfactory stem cells in the aged OE have reduced responses to the trophic factors NPY and ATP as measured by basal cell proliferation. In fact, a higher concentration of NPY was required to significantly increase proliferation. These data suggest that aging not only leads to downregulation of NPY protein but also impairs NPY signaling at the olfactory stem cell level in the OE. Examination of OE tissue and proliferation in the IP3R3$^{-/-}$ mouse indicated that IP3R3/NPY signaling has no effect on the aforementioned age-related decline in tissue homeostasis. However, the ability to upregulate proliferation following toxicant injury is compromised in the OE of aged IP3R3$^{-/-}$ mouse. These data indicate that IP3R3/NPY signaling plays a role in injury-induced recovery in the aged mouse.

4.1. Age-related alterations in OE tissue homeostasis

Olfactory basal stem cell proliferation and neuronal differentiation in the OE is tightly regulated by environmental signals derived from a niche defined by the extracellular matrix of the basement membrane, growth factors released by surrounding cells, and the nearby vasculature (Mackay-Sim and Chuah, 2000). Despite the remarkable ability to regenerate, impairment of OE homeostasis occurs with time that may be caused by both extrinsic mechanisms, such as cumulative damage from environmental pollutants and disease, and intrinsic mechanisms, such as a reduction in trophic factor levels or stem cell populations.

The anterior and more exposed portion of the OE is more damaged than the posterior OE in aged animals, suggesting that cumulative environmental insults may contribute to age-related changes in tissue homeostasis (Loo et al., 1996). However, age-related decreases in cell density can also be observed in the more protected posterior OE (Lee et al., 2009, Loo et al., 1996). Additionally, the number of neurons undergoing apoptosis in the OE decreases with age, suggesting that the turnover rate of neurons in the aged mouse is slower than in the younger mouse (Kondo et al., 2010). The IP3R3^{+} microvillous cells are resistant to bulbectomy-induced neuronal apoptosis (Jia et al., 2013), and are likely derived from olfactory stem cell proliferation and differentiation, and have a slow turnover rate (Pfister et al., 2012). A previous study reported that aged rat OE microvillous cells morphologically similar to IP3R3^{+} microvillous cells had marked hypertrophy but were resistant to age-

related reductions in cell number compared to other OE cell types (Kwon et al., 2005). In the present study, using a transgenic IP3R3-tauGFP mouse we found age-dependent reductions in $IP3R3^+$ cells and NPY^+ cells but seldom observed hypertrophy of $IP3R3^+$ microvillous cells in aged mouse OE.

Decreased trophic factor expression is correlated to alterations in tissue homeostasis. Waved-1 mutant mice have low levels of transforming growth factor-α and phenocopy aged mice in proliferation rates and olfactory dysfunction (Enwere et al., 2004). Here, in the posterior OE of aged mice, we found that the numbers of $IP3R3^+$ microvillous cells were significantly reduced at 12 and 24 months, and the number of NPY^+ cells and NPY protein level were significantly decreased at 24 months in the OE of $IP3R3^{+/-}$ mice. Consistent with these data, the numbers of olfactory stem cells, proliferating stem cells, olfactory sensory neurons and olfactory-mediated functions were significantly reduced in 24 month old $IP3R3^{+/-}$ mice. A similar reduction in stem cell numbers in the OE of young $NPY^{-/-}$ and NPY $Y_1^{-/-}$ mice was observed (Doyle et al., 2008, Hansel et al., 2001). These data suggested that age-dependent downregulation of NPY may contribute to the age-related declines of OE tissue homeostasis. Interestingly, in our study the levels of NPY mRNA were not altered over 24 months. Age-related post-translational protein modifications are common and have been linked to age-related diseases including neurodegenerative diseases (Grillo and Colombatto, 2008, Soskic et al., 2008). A methionine residue in NPY is increasingly oxidized in rat adrenal glands over time (Higuchi et al., 1988). The age-related increase in the level of oxidized methionine in NPY may contribute to our observation in a decrease in NPY levels, yet stable level of NPY mRNA.

The age-dependent decrease in olfactory stem cell proliferation in the OE could also be due to a reduction in calcium-dependent NPY release or a reduced sensitivity of olfactory stem cells to NPY. Calcium homeostasis is altered during aging, which can detrimentally affect calcium-dependent trophic factor secretion (Lin et al., 2007). Additional support is the fact that increasing the concentration of exogenous NPY increased proliferation in OE tissue in 12 month mice and that ATP is no longer able to promote basal cell proliferation in the OE of 24 month mice. These data suggest that the basal cells in aged OE have low sensitivity to NPY stimulation.

Finally, the reduced number of $MASH1^+$ globose basal cells and $CK5^+$ horizontal basal cells could cause the age-related decrease in stem cell proliferation. In our $IP3R3^{-/-}$ mice model in which IP3R3-mediated NPY release is impaired, we do find decreased numbers of olfactory stem cells in the OE at 2 months (Jia et al., 2013). However, there is no alteration in basal cell proliferation and olfactory sensory neuron numbers in 2 month $IP3R3^{-/-}$ mice (Jia et al., 2013). Moreover, there are no further decreases in olfactory stem cells, proliferating stem cells, olfactory sensory neurons and olfactory-mediated functions in 12 and 24 months OE of $IP3R3^{-/-}$mice when compared to age-matched $IP3R3^{+/-}$ mice. These data suggest IP3R3-mediated NPY release contributes to maintenance of the population of olfactory stem cells at 2 months, a developmental stage when the surface area of OE is still increasing in mouse (Hinds and McNelly, 1981), but is not involved in age-related declines in OE tissue homeostasis under physiological conditions. There may be multiple intrinsic trophic factors that work concertedly to regulate tissue homeostasis.

4.2. Aged-related decline in olfactory function

Olfaction deficits occur with age in humans (Stevens and Cain, 1987) in 50% and 75% of the population over 65 and 80 years, respectively (Murphy et al., 2002). Age-related loss of olfactory function has also been observed in rodents, which makes rodents a good model for studying the aging process in olfactory system (Enwere et al., 2004). Using patch clamp recordings on single neurons, Lee et al. (2009) showed that the OSNs from aged mice (24–27 months) display similar response amplitudes and sensitivities to a single tested odorant as compared to those from younger adults, indicating individual OSNs retain their sensitivity to odorants. Likewise, the expression of 531 odorant receptor genes is stable between the ages of 2 and 31 months in C57Bl/6 mice (Khan et al., 2013). Functional decline in olfaction could be related to changes in the structure of olfactory system. Olfaction is defined by olfactory threshold, identification and discrimination. Olfactory threshold is likely to be influenced by the peripheral OE, while odorant identification and discrimination are influenced by the central olfactory structures, the olfactory bulb and cortex (Enwere et al., 2004, Kovacs, 2004). The age-related olfactory decline is marked as an elevation of threshold and a diminished sensitivity to suprathreshold stimuli, e.g., compared to the young subject, the elderly perceive a given odorant as less intense and have a reduced ability to identify it (Loo et al., 1996, Patel and Larson, 2009). These data indicate that age-related olfaction decline may be mainly due to changes in the peripheral OE, however, changes in olfactory bulb and cortex cannot be excluded (Hinds and McNelly, 1981, Mobley et al., 2013).

This study used the buried food test: the first trial measures the ability to smell via naïve olfactory-mediated behavior and the subsequent trials measure olfactory-mediated learning and memory by measuring the ability to improve based on the positive reinforcements from previous trials (Le Pichon et al., 2009). The results of this assay indicated that (1) smell perception is impaired in aged mice, probably due to the 15% loss of OSNs in the OE and loss of OSN axons in the olfactory bulb of 24 month mice, and (2) olfactory-mediated learning and memory are impaired, suggesting that the olfactory bulb and cortex are also affected in aging. The olfactory habituation/dishabituation test was used to examine novel odorant investigation, odorant discrimination and odorant habituation. Both 24 month $IP3R3^{+/-}$ and $IP3R3^{-/-}$ mice showed reduced novel odorant investigation and odorant discrimination, consistent with the data from buried food test. This was observed using a high concentration of odorants (1:100) to eliminate any potential differences in sensitivity that may arise from degeneration of the OE with age. Our data, suggesting that the reduced sensitivity to odorants, possibly due to loss of OSNs in the aged OE and olfactory bulb, may contribute to the difficulty in novel odorant investigation and discrimination in aged mice. Indeed, in a senescence-accelerated mouse model, olfactory sensitivity measured by electroolfactogram and behavioral tests decreases dramatically with age due to loss in the number of OSNs (Nakayasu et al., 2000). A single sniff of an odorant is sufficient for detection and discrimination (Wesson et al., 2008), while prolonged sniffing response is an indicator of arousal and motivation (Wachowiak et al., 2009). Therefore, the reduced novel odorant investigation we observed in aged mice may also be due to less arousal and motivation. Finally, there are no significant alterations in odorant habituation from 2 to 24

month old mice. These data suggest that the mechanism of olfactory adaption may be preserved through ages.

4.3. The role of IP3R3 and NPY on age-related impairment of injury-induced regeneration

Very few studies have examined possible ways to improve recovery following injury. Herzog and Otto established that subcutaneous administration of fibroblast growth factor 2, epidermal growth factor, or transforming growth factor a increased the reinnervation of the olfactory bulb following $ZnSO_4$ toxicant treatment (Herzog and Otto, 1999). Transforming growth factor a also enhanced the rate of recovery following olfactory nerve transection measured by an odorant-guided fear conditioning assay (Herzog and Otto, 2002). Neither study examined the olfactory system past 10 days post-injury, the earliest time a mature neuron could be generated following damage. Yee and Rawson determined that oral administration of retinoic acid 1 day post-transection enhanced recovery at 16 days post-transection as measured using the buried food assay (Yee and Rawson, 2000). To date, no study investigating potential therapeutics has evaluated the effects of age on recovery.

Our previous studies demonstrated in young (2 month) mice that maintenance of the population of olfactory stem cells and their proliferation following injury are dependent, in part, on IP3R3-mediated secretion of the neurotrophic factor NPY from $IP3R3^{+}$ microvillous cells (Jia et al., 2013). Here, we show that the proliferative response following injury (driven by bulbectomy and olfactotoxicant) decreases with age in the $IP3R3^{+/-}$ mice. We speculate that the observed IP3R3-independent age-related decrease in olfactory stem cells underlies this response. We used the $IP3R3^{-/-}$ mouse to examine the effect of ATP-dependent NPY secretion on the regenerative response to injury. With the ATP-independent bulbectomy injury model, there was no difference in the proliferative response between $IP3R3^{+/-}$ and $IP3R3^{-/-}$ mice. In contrast, $IP3R3^{-/-}$ mice have a decreased proliferative response to injury driven by an olfactotoxicant that elicits ATP dependent release of NPY. These different injury models induce different signaling cascades. Multiple signaling mechanisms leading to regeneration may exist to account for different forms of injury. Here we demonstrate that a deficiency in IP3R3-mediated NPY release, either due to age, genetics or both, impairs the proliferative response to an olfactotoxicant. These data indicate that IP3R3/NPY signaling plays a role in injury-induced OE recovery in aged mouse. This study provides an underlying mechanism for the reduced efficiency of responding to toxicant insult in the elderly.

Acknowledgements

Research was supported by NIH DC006897 and MSU institutional funds. We thank Brian Jespersen, and the Pharmacology and Toxicology Departmental Core Facilities for technical support.

Abbreviations

OE	olfactory epithelium
IP3R3	inositol trisphosphate receptor type 3
NPY	neuropeptide Y

BrdU	bromodeoxyuridine
MASH1	mammalian achaete-scute complex homolog-1
CK5	cytokeratin 5
OMP	olfactory marker protein
SG	satratoxin G

References

Caggiano M, Kauer JS, Hunter DD. Globose basal cells are neuronal progenitors in the olfactory epithelium: a lineage analysis using a replication-incompetent retrovirus. Neuron. 1994; 13(2):339–352. [PubMed: 8060615]

Calof AL, Chikaraishi DM. Analysis of neurogenesis in a mammalian neuroepithelium: proliferation and differentiation of an olfactory neuron precursor in vitro. Neuron. 1989; 3(1):115–127. [PubMed: 2482777]

Doyle KL, Karl T, Hort Y, Duffy L, Shine J, Herzog H. Y1 receptors are critical for the proliferation of adult mouse precursor cells in the olfactory neuroepithelium. J Neurochem. 2008; 105(3):641–652. [PubMed: 18088353]

Enwere E, Shingo T, Gregg C, Fujikawa H, Ohta S, Weiss S. Aging results in reduced epidermal growth factor receptor signaling, diminished olfactory neurogenesis, and deficits in fine olfactory discrimination. J Neurosci. 2004; 24(38):8354–8365. [PubMed: 15385618]

Graziadei, PPC.; Monti-Graziadei, GA. Continuous nerve cell renewal in the olfactory system. In: Jacobson, M., editor. Handbook of Sensory Physiology. New York: Springer; 1978. p. 55-83.

Grillo MA, Colombatto S. Advanced glycation end-products (AGEs): involvement in aging and in neurodegenerative diseases. Amino acids. 2008; 35(1):29–36. [PubMed: 18008028]

Hansel DE, Eipper BA, Ronnett GV. Neuropeptide Y functions as a neuroproliferative factor. Nature. 2001; 410(6831):940–944. [PubMed: 11309620]

Hegg CC, Jia C, Chick WS, Restrepo D, Hansen A. Microvillous cells expressing IP3R3 in the olfactory epithelium of mice. Eur J Neurosci. 2010; 32(10):1632–1645. [PubMed: 20958798]

Herzog C, Otto T. Regeneration of olfactory receptor neurons following chemical lesion: time course and enhancement with growth factor administration. Brain Res. 1999; 849(1–2):155–161. [PubMed: 10592297]

Herzog CD, Otto T. Administration of transforming growth factor-alpha enhances anatomical and behavioral recovery following olfactory nerve transection. Neuroscience. 2002; 113(3):569–580. [PubMed: 12150777]

Higuchi H, Yang HY, Costa E. Age-related bidirectional changes in neuropeptide Y peptides in rat adrenal glands, brain, and blood. J Neurochem. 1988; 50(6):1879–1886. [PubMed: 3373217]

Hinds JW, McNelly NA. Aging in the rat olfactory system: correlation of changes in the olfactory epithelium and olfactory bulb. J Comp Neurol. 1981; 203(3):441–453. [PubMed: 7320235]

Jia C, Doherty JD, Crudgington S, Hegg CC. Activation of purinergic receptors induces proliferation and neuronal differentiation in Swiss Webster mouse olfactory epithelium. Neuroscience. 2009; 163(1):120–128. [PubMed: 19555741]

Jia C, Hayoz S, Hutch CR, Iqbal TR, Pooley AE, Hegg CC. An IP3R3- and NPY-expressing microvillous cell mediates tissue homeostasis and regeneration in the mouse olfactory epithelium. PLoS One. 2013; 8(3):e58668. [PubMed: 23516531]

Jia C, Hegg CC. Neuropeptide Y and extracellular signal-regulated kinase mediate injury-induced neuroregeneration in mouse olfactory epithelium. Mol Cell Neurosci. 2012; 49(2):158–170. [PubMed: 22154958]

Jia C, Roman C, Hegg CC. Nickel sulfate induces location-dependent atrophy of mouse olfactory epithelium: protective and proliferative role of purinergic receptor activation. Toxicol Sci. 2010; 115(2):547–556. [PubMed: 20200219]

Jia C, Sangsiri S, Belock B, Iqbal T, Pestka JJ, Hegg CC. ATP mediates neuroprotective and neuroproliferative effects in mouse olfactory epithelium following exposure to satratoxin G in vitro and in vivo. Toxicol Sci. 2011; 124(1):169–178. [PubMed: 21865290]

Kanekar S, Jia C, Hegg CC. Purinergic receptor activation evokes neurotrophic factor neuropeptide Y release from neonatal mouse olfactory epithelial slices. J Neurosci Res. 2009; 87(6):1424–1434. [PubMed: 19115410]

Khan M, Vaes E, Mombaerts P. Temporal patterns of odorant receptor gene expression in adult and aged mice. Mol Cell Neurosci. 2013; 57:120–129. [PubMed: 23962816]

Kondo K, Suzukawa K, Sakamoto T, Watanabe K, Kanaya K, Ushio M, Yamaguchi T, Nibu K, Kaga K, Yamasoba T. Age-related changes in cell dynamics of the postnatal mouse olfactory neuroepithelium: cell proliferation, neuronal differentiation, and cell death. J Comp Neurol. 2010; 518(11):1962–1975. [PubMed: 20394053]

Kovacs T. Mechanisms of olfactory dysfunction in aging and neurodegenerative disorders. Ageing Res Rev. 2004; 3(2):215–232. [PubMed: 15177056]

Kwon BS, Kim MK, Kim WH, Pyo JS, Cheon YH, Cha CI, Nam SY, Baik TK, Lee BL. Age-related changes in microvillar cells of rat olfactory epithelium. Neurosci Lett. 2005; 378(2):65–69. [PubMed: 15774259]

Le Pichon CE, Valley MT, Polymenidou M, Chesler AT, Sagdullaev BT, Aguzzi A, Firestein S. Olfactory behavior and physiology are disrupted in prion protein knockout mice. Nat Neurosci. 2009; 12(1):60–69. [PubMed: 19098904]

Lee A, Tian H, Grosmaitre X, Ma M. Expression patterns of odorant receptors and response properties of olfactory sensory neurons in aged mice. Chem Senses. 2009; 34(8):695–703. [PubMed: 19759360]

Leung CT, Coulombe PA, Reed RR. Contribution of olfactory neural stem cells to tissue maintenance and regeneration. Nat Neurosci. 2007; 10(6):720–726. [PubMed: 17468753]

Lin DT, Wu J, Holstein D, Upadhyay G, Rourk W, Muller E, Lechleiter JD. Ca2+ signaling, mitochondria and sensitivity to oxidative stress in aging astrocytes. Neurobiol Aging. 2007; 28(1): 99–111. [PubMed: 16359757]

Loo AT, Youngentob SL, Kent PF, Schwob JE. The aging olfactory epithelium: neurogenesis, response to damage, and odorant-induced activity. International journal of developmental neuroscience : the official journal of the International Society for Developmental Neuroscience. 1996; 14(7–8):881–900. [PubMed: 9010732]

Mackay-Sim A, Chuah MI. Neurotrophic factors in the primary olfactory pathway. Prog Neurobiol. 2000; 62:527–559. [PubMed: 10869782]

Mobley AS, Bryant AK, Richard MB, Brann JH, Firestein SJ, Greer CA. Age-dependent regional changes in the rostral migratory stream. Neurobiol Aging. 2013; 34(7):1873–1881. [PubMed: 23419702]

Montani G, Tonelli S, Elsaesser R, Paysan J, Tirindelli R. Neuropeptide Y in the olfactory microvillar cells. Eur J Neurosci. 2006; 24(1):20–24. [PubMed: 16800866]

Murphy C, Schubert CR, Cruickshanks KJ, Klein BE, Klein R, Nondahl DM. Prevalence of olfactory impairment in older adults. JAMA. 2002; 288(18):2307–2312. [PubMed: 12425708]

Naguro T, Iwashita K. Olfactory epithelium in young adult and aging rats as seen with high-resolution scanning electron microscopy. Microsc Res Tech. 1992; 23(1):62–75. [PubMed: 1392072]

Nakayasu C, Kanemura F, Hirano Y, Shimizu Y, Tonosaki K. Sensitivity of the olfactory sense declines with the aging in senescence-accelerated mouse (SAM-P1). Physiol Behav. 2000; 70(1–2):135–139. [PubMed: 10978488]

Patel RC, Larson J. Impaired olfactory discrimination learning and decreased olfactory sensitivity in aged C57Bl/6 mice. Neurobiol Aging. 2009; 30(5):829–837. [PubMed: 17904696]

Pfister S, Dietrich MG, Sidler C, Fritschy JM, Knuesel I, Elsaesser R. Characterization and turnover of CD73/IP(3)R3-positive microvillar cells in the adult mouse olfactory epithelium. Chem Senses. 2012; 37(9):859–868. [PubMed: 22952298]

Schwartz Levey M, Chikaraishi DM, Kauer JS. Characterization of potential precursor populations in the mouse olfactory epithelium using immunocytochemistry and autoradiography. J Neurosci. 1991; 11:3556–3564. [PubMed: 1719164]

Schwob JE, Huard JM, Luskin MB, Youngentob SL. Retroviral lineage studies of the rat olfactory epithelium. Chem Senses. 1994; 19(6):671–682. [PubMed: 7735846]

Soskic V, Groebe K, Schrattenholz A. Nonenzymatic posttranslational protein modifications in ageing. Experimental gerontology. 2008; 43(4):247–257. [PubMed: 18215483]

Stevens JC, Cain WS. Old-age deficits in the sense of smell as gauged by thresholds, magnitude matching, and odor identification. Psychol Aging. 1987; 2(1):36–42. [PubMed: 3268190]

Tschanz SA, Burri PH, Weibel ER. A simple tool for stereological assessment of digital images: the STEPanizer. Journal of microscopy. 2011; 243(1):47–59. [PubMed: 21375529]

Wachowiak M, Wesson DW, Pirez N, Verhagen JV, Carey RM. Low-level mechanisms for processing odor information in the behaving animal. Ann N Y Acad Sci. 2009; 1170:286–292. [PubMed: 19686149]

Weiler E, Farbman AI. Proliferation in the rat olfactory epithelium: age-dependent changes. J Neurosci. 1997; 17(10):3610–3622. [PubMed: 9133384]

Weiler E, Farbman AI. Supporting cell proliferation in the olfactory epithelium decreases postnatally. Glia. 1998; 22(4):315–328. [PubMed: 9517564]

Wesson DW, Donahou TN, Johnson MO, Wachowiak M. Sniffing behavior of mice during performance in odor-guided tasks. Chem Senses. 2008; 33(7):581–596. [PubMed: 18534995]

Won MH, Kang TC, Lee JC, Choi KY, Park SK, Jeong YG, Jo SM. Age-related change of neuropeptide Y-immunoreactive neurons in the rat main olfactory bulb. Neurosci Lett. 2000; 289(2):119–122. [PubMed: 10904134]

Yee KK, Rawson NE. Retinoic acid enhances the rate of olfactory recovery after olfactory nerve transection. Brain Res Dev Brain Res. 2000; 124(1–2):129–132.

- IP3R3$^{-/-}$ mice were used to study IP3R3/NPY signaling, aging and olfactory function
- Aging downregulates NPY protein and impairs NPY signaling to olfactory stem cells
- IP3R3 deficiency did not cause further impairment of normal stem cell proliferation
- Proliferation following toxicant injury is compromised in aged IP3R3$^{-/-}$ mouse.
- IP3R3/NPY signaling plays a role in injury-induced recovery in the aged mouse

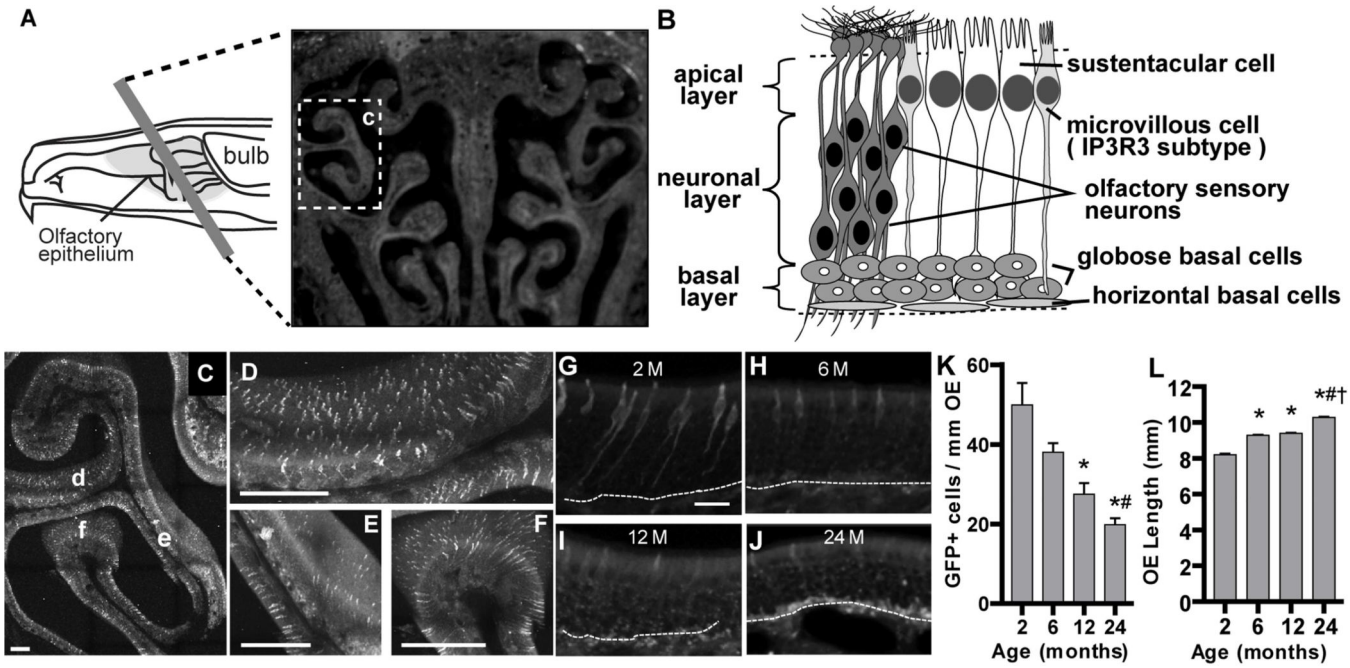

Figure 1. The number of IP3R3^{+} cells decreases with age in the OE of IP3R3$^{+/-}$ mice

(**A**) Schematic showing hemisection of the nasal cavity (left panel) and a representative image of a coronal tissue section (right panel). Box labeled c indicates the ectoturbinate 2 region shown in C. (**B**) Schematic cross section of the olfactory epithelium indicating the 3 layers (left) and representations of the different cell types (right). (**C–F**) A 200 μm coronal OE section from a 2 month old IP3R3$^{+/-}$ mouse was scanned for GFP^{+} cells using 2-photon confocal microscopy. (C) A low power representative image shows even distribution of GFP-labeled IP3R3^{+} cells in the OE of ectoturbinate 2. Higher magnification of regions denoted d–f is shown in D–F, respectively. Scale bar = 200 μm. (**G–J**) Representative images of GFP-labeled IP3R3^{+} cells in the OE of IP3R3$^{+/-}$ mice at 2, 6, 12 and 24 months. Dashed line marks the basement membrane. Scale bar = 20 μm. (**K**) Bar graph depicting the number of GFP^{+} cells in the ectoturbinate 2 and endoturbinate II of OE from IP3R3$^{+/-}$ mice at 2, 6, 12 and 24 months. * $p < 0.05$ at 2 vs. 6, 12 and 24 months, # $p < 0.05$ at 6 vs. 24 months (one-way ANOVA followed by Newman-Keuls post-hoc test; n = 5, 5, 3 and 4 mice, respectively). (**L**) Bar graph of the length of ectoturbinate 2 and endoturbinate II OE measured along the basement membrane in IP3R3$^{+/-}$ mice aged 2, 6, 12 and 24 months. * $p < 0.001$ at 2 vs. 6, 12 and 24 months, # $p < 0.001$ at 6 vs. 24 months, † $p < 0.001$ at 12 vs. 24 months (one-way ANOVA followed by Newman-Keuls post-hoc test; n = 4, 6, 6 and 5 mice, respectively).

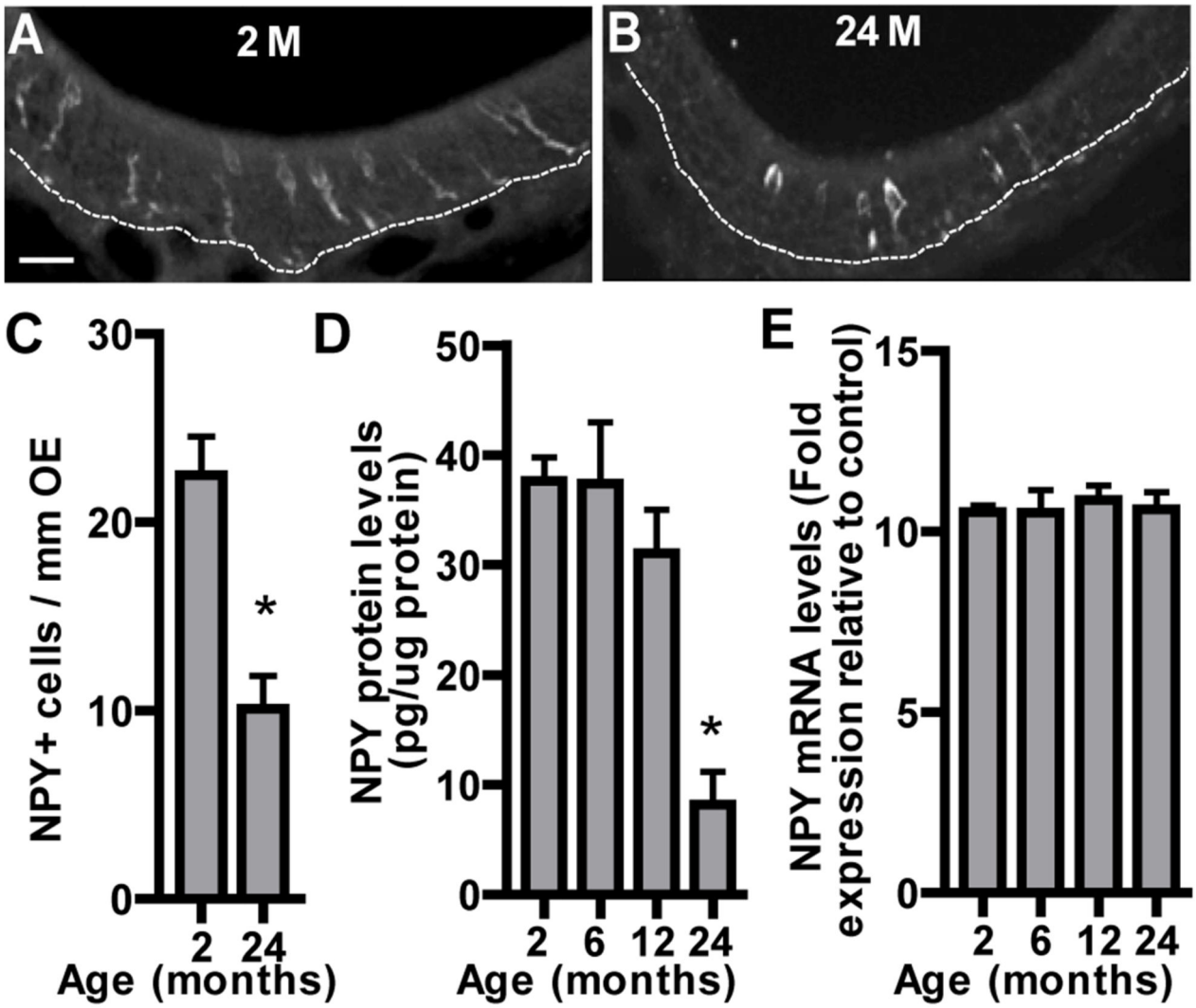

Figure 2. Age reduces NPY^{+} cells and NPY protein in mouse OE

(**A–B**) Representative images of NPY-immunoreactive cells in the OE of IP3R3$^{+/-}$ mice at 2 and 24 months. Scale bar = 20 μm. (**C**) The number of NPY^{+} cells is significantly reduced in the ectoturbinate 2 and endoturbinate II OE of IP3R3$^{+/-}$ mice at 24 vs. 2 months. * $p < 0.05$ (Student's T test, n = 4 and 6 mice, respectively). (**D**) The NPY protein level is significantly reduced in the OE of IP3R3$^{+/-}$ mice at 24 months compared to 2 months. * $p < 0.01$ vs. 2, 6 and 12 months (one-way ANOVA followed by Newman-Keuls post-hoc test; n = 4 mice per group). (**E**) The NPY mRNA levels in the OE of IP3R3$^{+/-}$ mice are comparable among all ages checked. $p > 0.05$ (one-way ANOVA followed by Newman-Keuls post-hoc test; n = 4 mice per group).

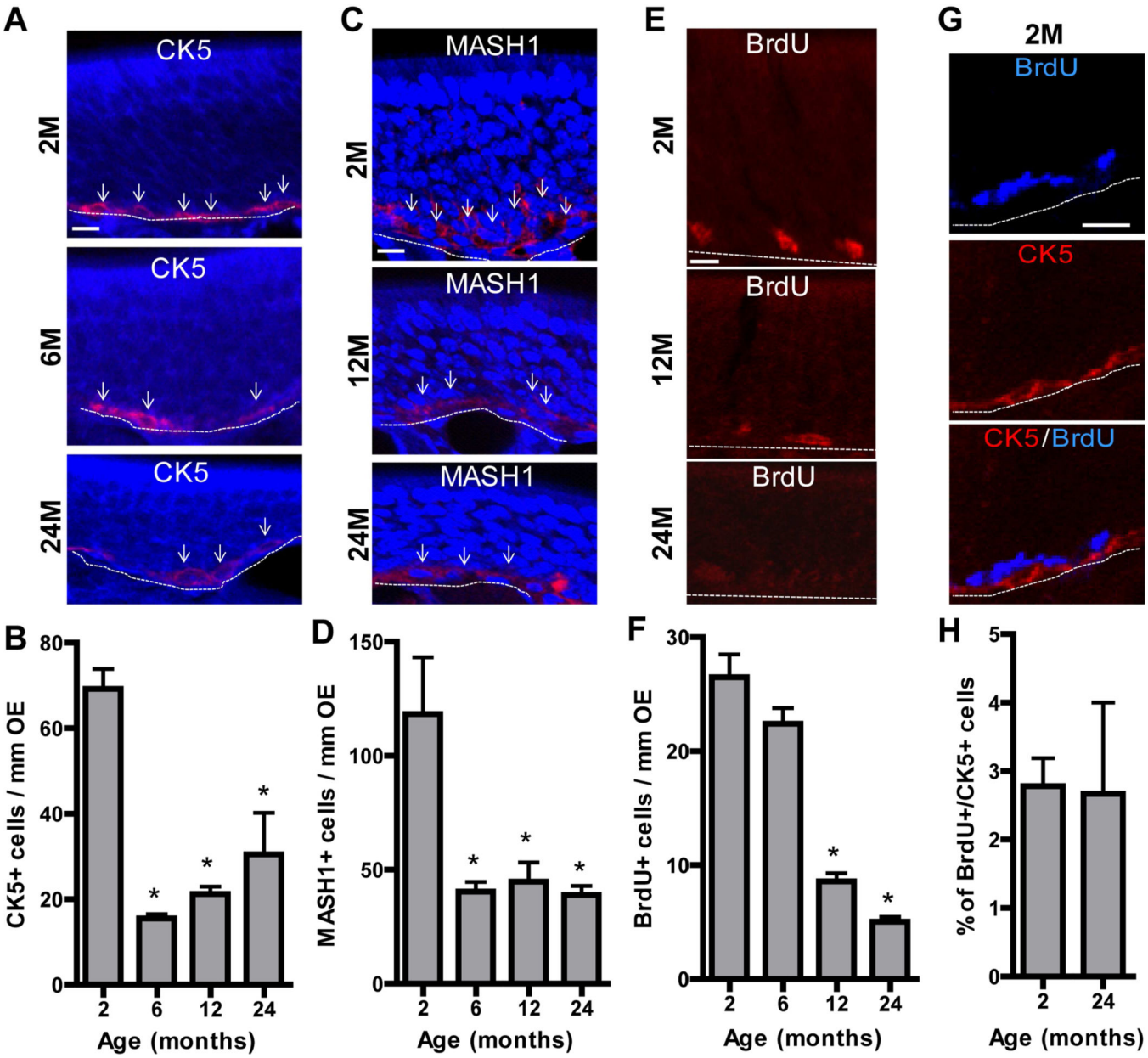

Figure 3. Age reduces basal cells and basal cell proliferation in mouse OE

(**A–D**) Representative immunoreactivity (red) to (A) CK5 (a marker for horizontal basal cells) and (C) MASH1 (a marker for globose basal cells) in the OE of IP3R3$^{+/-}$ at 2, 6, 12 and 24 months. Nuclei were counterstained with DAPI (blue). Dashed line marks the basement membrane. Arrows indicate representative immunoreactivity positive cells. Scale bar = 10 μm. The numbers of (B) CK5^{+} horizontal basal cells and (D) MASH1^{+} globose basal cells in the OE of IP3R3$^{+/-}$mice were significantly reduced from 2 to 6 months and then constant through 24 months. * $p < 0.01$ or 0.05, vs. 2 months respectively (one-way ANOVA followed by Newman-Keuls post-hoc test; n = 3 mice per group) (**E–F**) The rates of basal cell proliferation measured by BrdU incorporation were significantly reduced in the OE of IP3R3$^{+/-}$ mice at 12 and 24 months. * $p < 0.001$, vs. 2 and 6 months (one-way

ANOVA followed by Newman-Keuls post-hoc test; n = 3 mice per group). (**G**) Representative co-immunoreactivity to BrdU (blue) and CK5 (red) in the OE of 2 month old IP3R3$^{+/-}$ mice. Dashed line marks the basement membrane. Scale bar = 20 μm. (**H**) There is a low percentage of BrdU+ cells in the OE of 2 and 24 month old IP3R3$^{+/-}$ mice that colocalize with horizontal basal cell marker CK5 ($p>0.05$, Student's T test).

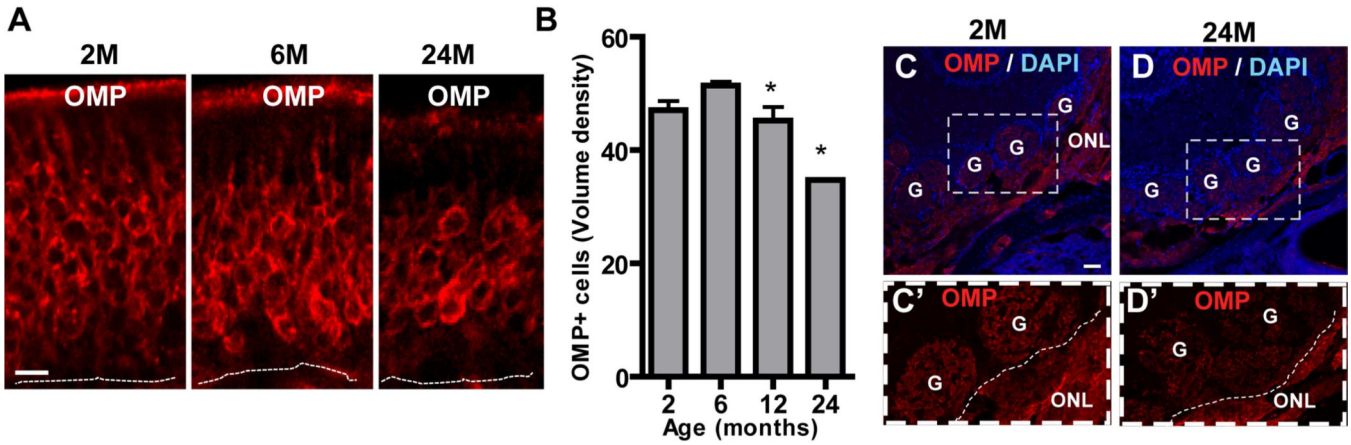

Figure 4. Age reduces olfactory sensory neurons in the OE and olfactory bulb

(**A**) Representative immunoreactivity to olfactory marker protein (OMP), a marker of mature olfactory sensory neurons, in the OE of IP3R3$^{+/-}$ mice at 2, 6, and 24 months. Dashed line marks the basement membrane. Scale bar = 10 μm. (**B**) The volume density of OMP^{+} neurons was significantly reduced in the OE of IP3R3$^{+/-}$ at 12 and 24 months. * $p < 0.001$ at 24 vs. 2, 6 and 12 months and $p < 0.01$ at 12 vs. 6 months (one-way ANOVA followed by Newman-Keuls post-hoc test; n = 3–6 mice per group). (**C–D**) Low (C–D) and high (C', D') magnification images depicting representative immunoreactivity to OMP in the olfactory bulb of IP3R3$^{+/-}$ mice at 2 (C, C') and 24 (D,D') months. Regions of higher magnification indicated by outlined region (white box). Nuclei were counterstained with DAPI. Dashed line marks the boundary between olfactory nerve layer (ONL) and glomerular layer (G). Scale bar = 50 μm.

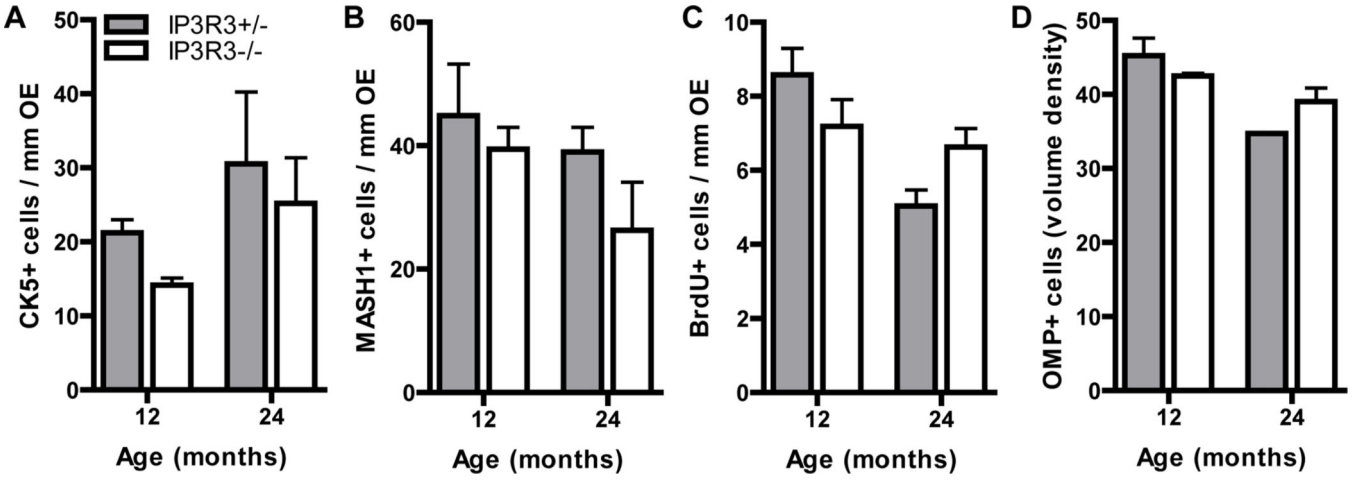

Figure 5. Cell populations and proliferation in aged OE of IP3R3$^{+/-}$ and IP3R3$^{-/-}$ mice

The numbers of (**A**) CK5^{+} horizontal basal cells and (**B**) MASH1^{+} globose basal cells in the OE of 12 and 24 month IP3R3$^{+/-}$ and IP3R3$^{-/-}$ mice were comparable. The rates of basal cell proliferation (**C**) measured by BrdU incorporation were not altered in the OE of IP3R3$^{+/-}$ and IP3R3$^{-/-}$ mice at 12 and 24 months. The volume density of OMP^{+} neurons (**D**) was not changed in the OE of IP3R3$^{+/-}$ and IP3R3$^{-/-}$ mice at 12 and 24 months. $P > 0.05$; Two-way ANOVA followed by Tukey/Kramer Procedure post-hoc test; n = 3–6 mice per group.

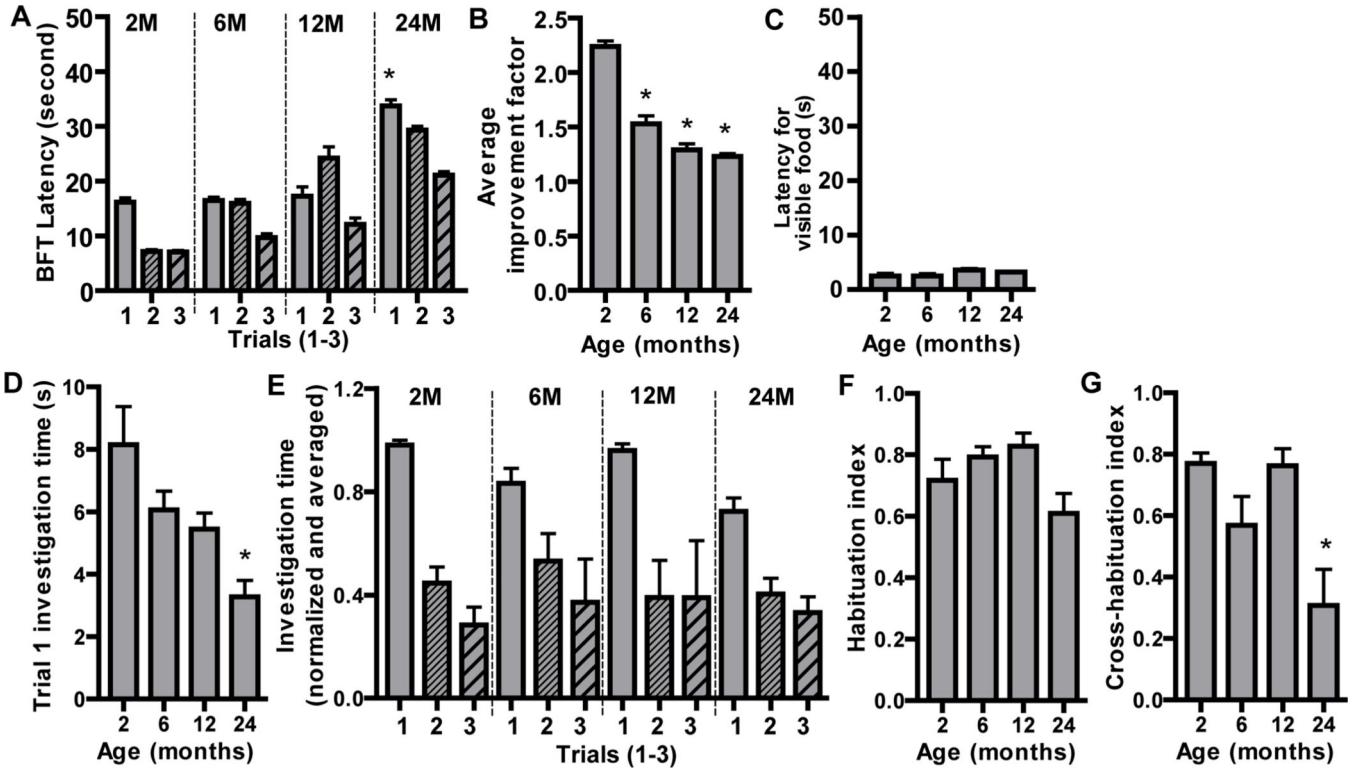

Figure 6. Age-dependent reductions in olfactory-mediated functions

(**A–C**) Buried food behavioral tests were performed every other day in fasted IP3R3$^{+/-}$ mice at age 2, 6, 12 and 24 months. (A) Average latency of trials 1–3. *, $p < 0.01$ for trial 1 at 24 vs. 2, 6 and 12 months (Repeated measures two-way ANOVA followed by Tukey/Kramer Procedure post-hoc test; n = 12–16 mice per group). (B) Average improvement factor, an indicator of olfactory-mediated learning and memory, calculated as the ratio of trial 1 vs. trial 3 latencies. * $p < 0.05$ vs. 2 months (One-way ANOVA followed by Newman-Keuls post-hoc test; n = 12–16 mice per group). (C) Latency of trial 4 with visible food, an assessment of locomotor activity ($p > 0.05$, one-way ANOVA followed by Tukey/Kramer Procedure post-hoc test; n = 12–16 mice per group). (**D–G**) The olfactory habituation/dishabituation behavioral tests were performed in IP3R3$^{+/-}$ mice at age 2, 6, 12 and 24 months. (D) The investigation time of the trail 1 (the average for all three odorants) is reduced in 24 month old mice. * $p < 0.01$ or 0.05, vs. 2 and 6 months (One-way ANOVA followed by Newman-Keuls post-hoc test; n = 12–16 mice per group). (E) Normalized and averaged investigation times for trials 1–3 for three odorants are shown. All mice showed a decrease in investigation time during trial 2 and 3 (habituation) and an increase in investigation time to a novel odorant presentation (dishabituation). (F) The habituation index was comparable across ages ($p>0.05$, One-way ANOVA followed by Newman-Keuls post-hoc test; n = 12–16 mice per group). (G) The ability to discriminate between odorants, measured by the cross-habituation index, was reduced in 24 month mice. * $p < 0.05$ or 0.01, vs. 2 and 12 months, respectively (One-way ANOVA followed by Newman-Keuls post-hoc test; n = 12–16 mice per group).

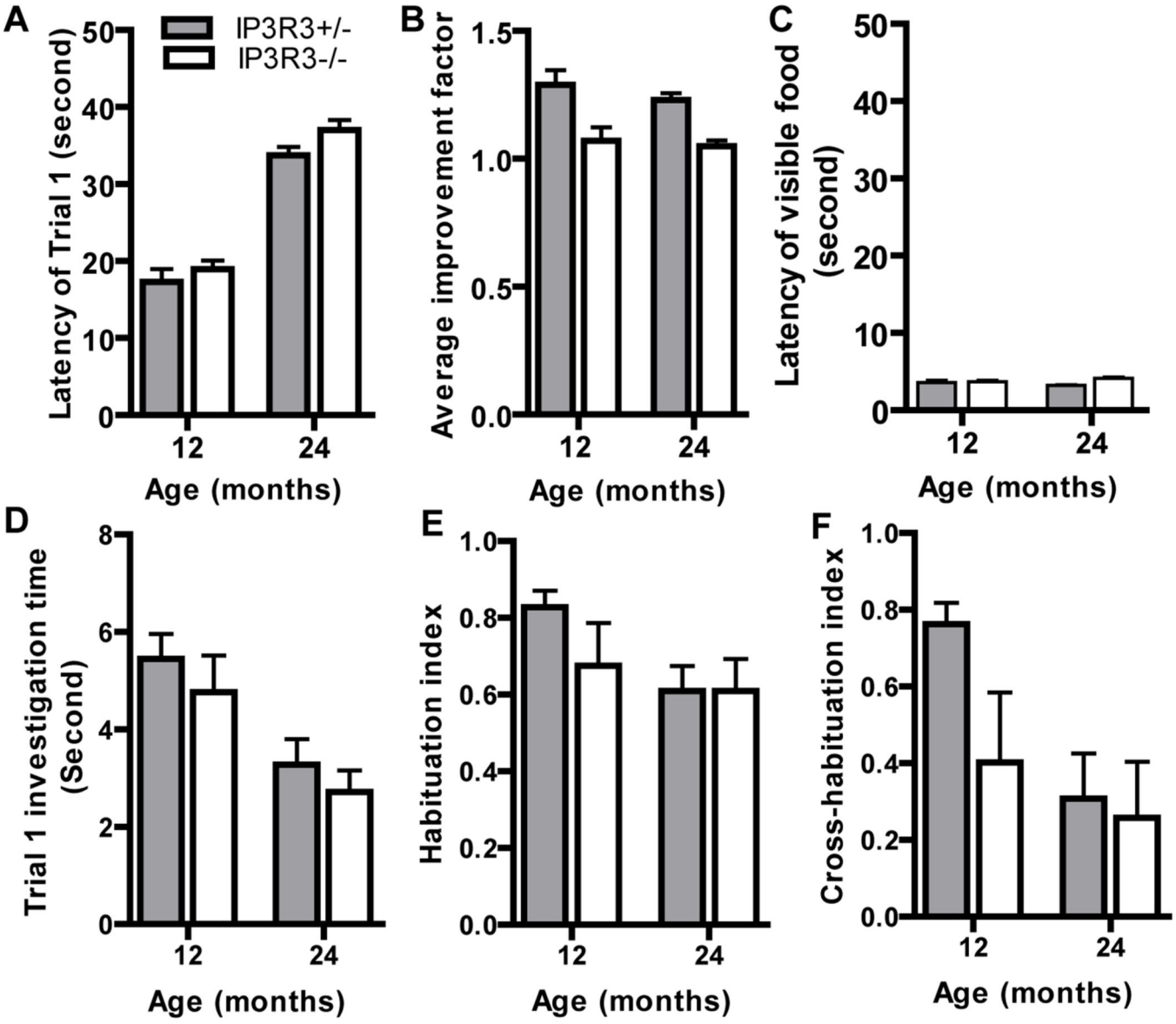

Figure 7. Olfactory-mediated behavior is not altered in aged IP3R3$^{+/-}$ and IP3R3$^{-/-}$ mice

The latencies of trial 1 (**A**), average improvement factors (**B**) and latencies of trial 4 with visible food (**C**) in buried food tests were comparable in 12 and 24 month IP3R3$^{+/-}$ and IP3R3$^{-/-}$ mice. The investigation time of trial 1 (**D**), habituation index (**E**) and cross-habituation index (**F**) in the olfactory habituation/dishabituation tests were not altered in 12 and 24 month IP3R3$^{+/-}$ and IP3R3$^{-/-}$ mice (Two-way ANOVA followed by Tukey/Kramer Procedure post-hoc test; n = 12–16 mice per group)

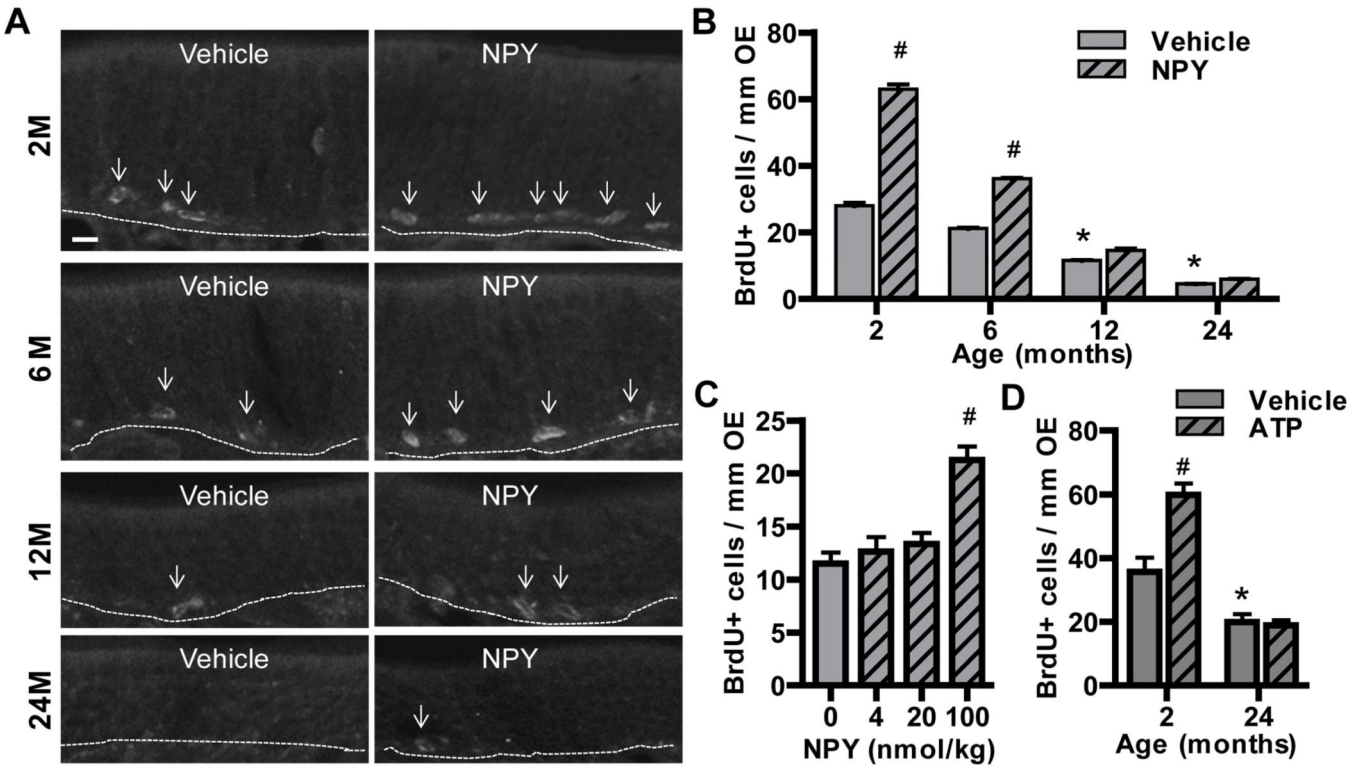

Figure 8. Trophic factor-stimulated basal cell proliferation is reduced in aged OE

IP3R3$^{+/-}$mice intranasally aspirated saline vehicle or NPY (4–100 nmol/kg) or ATP (400 nmol/kg) and the OE tissue was collected 2 days later. BrdU (total 144 mg/kg) was injected (i.p.) at 6 and 3 hours prior tissue collection. (**A**) Representative images of BrdU-labeled basal cells in the OE of IP3R3$^{+/-}$ mice treated with vehicle or NPY at 2, 6, 12, and 24 months. Scale bar = 10 μm. Arrows indicate BrdU^{+} basal cells. (**B**) NPY (4 nmol/kg) significantly increases BrdU^{+} basal cells in the OE of IP3R3$^{+/-}$ mice at 2 and 6 but not 12 and 24 months. # $p < 0.05$ vs. corresponding vehicle, * $p < 0.05$ vs. vehicle-treated 2 or 6 month mice (Two-way ANOVA followed by Tukey/Kramer Procedure post-hoc test; n = 3–6 mice per group). (**C**) The dose response of NPY (4, 20 and 100 nmol/kg) on basal cell proliferation in the OE of IP3R3$^{+/-}$ mice at 12 months. The number of BrdU^{+} basal cells was significantly increased with 100 nmol/kg NPY. * $p < 0.01$ vs. vehicle, 4 and 20 nmol/kg NPY (One-way ANOVA followed by Newman-Keuls post-hoc test; n = 3–4 mice per group). (**D**) ATP (400 nmol/kg) significantly increases BrdU^{+} basal cells in the OE of IP3R3$^{+/-}$ mice at 2 but not 24 months. # $p < 0.01$ vs. corresponding vehicle, * $p < 0.05$ vs. vehicle-treated 2 month mice (Two-way ANOVA followed by Tukey/Kramer Procedure post-hoc test; n = 3–6 mice per group).

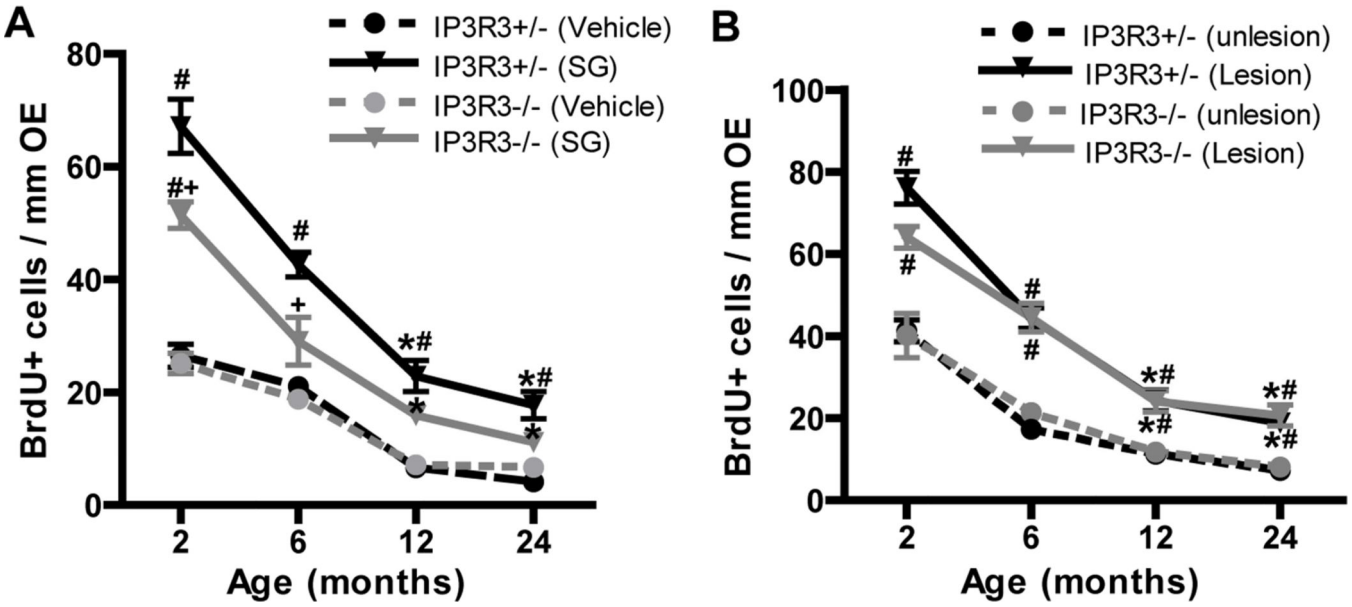

Figure 9. Regenerative response to injury is impaired in aged IP3R3$^{+/-}$ and IP3R3$^{-/-}$ mice

(**A**) IP3R3$^{+/-}$ and IP3R3$^{-/-}$ mice at 2, 6, 12 and 24 months intranasally aspirated vehicle saline or satratoxin G (SG; 100 μg/kg). BrdU (144 mg/kg, i.p.) was administered to mice at 6 and 3 hours prior to tissue collection at 6 days post-satratoxin G. Solid lines indicate satratoxin G-treated group and dashed lines indicate vehicle-treated group. *, $p < 0.01$ vs. satratoxin G-treated 2 and 6 month groups in the respective genotype; # $p < 0.01$ vs. vehicle in the respective IP3R3$^{+/-}$ and IP3R3$^{-/-}$ mice, + $p < 0.05$ vs. IP3R3$^{+/-}$ satratoxin G-treatment group (Two-way ANOVA followed by Turkey/Kramer Procedure post-hoc test; n = 3–6 mice per group). (**B**) Unilateral bulbectomy was performed in 2, 6, 12 and 24 month old IP3R3$^{+/-}$ and IP3R3$^{-/-}$ mice. BrdU (144 mg/kg) was given to mice at 6 and 3 hours prior to tissue collection at 6 days post-surgery. Solid lines indicate lesion side and dashed lines indicate unlesion side. *, $p < 0.01$ vs. lesion sides of 2 and 6 months in the respective genotype. #, $p < 0.05$ vs. unlesioned side in the respective IP3R3$^{+/-}$and IP3R3$^{-/-}$ mice (Two-way ANOVA followed by Turkey/Kramer Procedure post-hoc test; n = 3–6 mice per group).